Accepted Manuscript

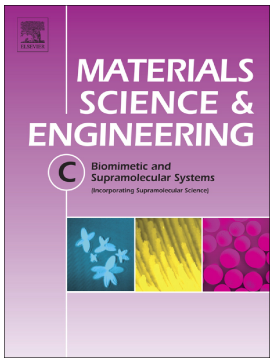

Cholesterol derived carbon quantum dots as fluorescence probe for the specific detection of hemoglobin in diluted human blood samples

Gopi Kalaiyarasan, James Joseph

PII: S0928-4931(18)30295-9
DOI: doi:10.1016/j.msec.2018.10.007
Reference: MSC 8933

To appear in: *Materials Science & Engineering C*

Received date: 29 January 2018
Revised date: 10 September 2018
Accepted date: 2 October 2018

Please cite this article as: Gopi Kalaiyarasan, James Joseph , Cholesterol derived carbon quantum dots as fluorescence probe for the specific detection of hemoglobin in diluted human blood samples. Msc (2018), doi:10.1016/j.msec.2018.10.007

Cholesterol derived carbon quantum dots as fluorescence probe for the specific detection of hemoglobin in diluted human blood samples

Gopi Kalaiyarasan[1, 2] and James Joseph[1, 2]*

[1]Acadamy of Scientific and Innovative Research (AcSIR), CSIR-Central Electrochemical Research Institute (CECRI) Campus, Karaikudi-630 003, India

[2]Electrodics and Electrocatalysis Division, CSIR-CECRI, Karaikudi-630 003, India

*Email: jameskavalam@yahoo.com, jamescecri@cecri.res.in

Abstract

In the current decade, carbon quantum dots (CQDs) are promising fluorescence probe in bio/analytical chemistry due to its unique properties. The functional groups of CQDs can be tuning the optical properties and selectively make a strong bond with target molecules. The interactions between Hb and cholesterol through hydrophobic batches are more favorable than the usual π-π interaction between CQDs and Hb. Hence we prepared highly stable CQDs with a fluorescence quantum yield of 45 % from cholesterol by the hydrothermal method to make hydrophobic interactions with Hb. Concurrently the CQDs possess graphitic crystalline and amphiphilic structure in nature. The fluorescence at 440 nm arises from the intrinsic core of CQDs and it will not affect by solution pH and excitation wavelengths. This fluorescence intensity was selectively quenched by Hb owing to the formation of fluorescence inactive complex (CQDs-Hb) through strong hydrophobic interactions. The quenching mechanism complies with the Forster non-radiative energy transfer (FRET) theory. This method shows good linearity from 0.1 μM to 2.9 μM with a limit of detection of 24 nM (S/N = 3). This observation is used for the quenchometric determination of Hb in diluted human blood samples.

Keywords biosensor, fluorescence quenching, carbon dots, hydrothermal method, photoluminescence.

1 Introduction

The fluorescent carbon quantum dots (CQDs) are a new class of carbon nanomaterial that has been developed in recent years. The CQDs have garnered much interest as prospective contenders to fluorescent metal nanoclusters (MNCs) and conventional semiconductor quantum dots (SQDs) due to its desired advantages of low cost, chemical inertness, high aqueous solubility, resistant to photobleaching, ease of synthesis, low toxicity, biocompatibility and environmental sociability[1]. The surface passivation and functionalization of CQDs allow the control of their physicochemical properties to demonstrate the strong bonding with target biomolecules[2]. In addition, we can tune the optical and physiochemical properties by altering the parameters of the reaction conditions such as the concentration of precursor, temperature, pH and time[3]. Therefore, the CQDs are favorable in the field of energy production and conversion, optoelectronic devices, biomedical applications like drug delivery, bioimaging and biosensor[4–6]. Recently Zhe Liu et al developed ultra-small fluorinated graphene materials as anti-cancer drug carrier for cancer therapeutics[6–8]. Jiu-Ju Feng et al developed carbon dots for sensing and imaging applications[9–11]. Numerous synthetic methods like chemical, electrochemical[12,13], arc discharge, laser ablation/passivation, plasma treatment[14], hydrothermal method[15], microwave[16], ultrasonic[17] have been established in the past decade to prepare fluorescent CQDs using various precursors including citrate[3], ascorbic acid[18], glucose[19], egg[14], orange juice[20] etc. Peiwei Gong et al prepared fluorinated graphene quantum dots from fluorinated graphite by gradient fluorine sacrifice strategy for enhancing formation and performance[21]. Generally, the unavoidable formation of the oxygen and oxygen-containing

functional groups in their structure offering the excitation-dependent fluorescence emission[18]. To get excitation independent fluorescence emission, researchers added phosphorus, nitrogen, and sulfur source along with precursor[9–11,22]. Un-doped, hydroxyl-rich CQDs with excitation independent fluorescence nature obtained in this work that is new.

Hemoglobin (Hb) is a metalloprotein which is present in red blood cells containing globin (protein part) and heme (conjugated structure with an iron(II) atom at the center and four porphyrin N atoms arranged at the corners of the face)[23,24]. Hb is essential to transport oxygen from the lungs to various parts and carbon dioxide from various parts to lungs. The Hb level in blood is related to numerous clinical diseases including leukemia, anemia, heart diseases, etc. The normal level of Hb for a male is 13.5–17.0 g/dL, for a female is 12.0–15.0 g/dL, for Pregnancy is 11.0-12.0 g/dL, for newborn is 14.0-24.0 g/dL and for children are 11.0-16.0 g/dL. Yearly 2 billion people affected worldwide including women and children with anemia due to insufficient Hb level in blood. Therefore accurate determination of Hb in blood for medical diagnosis is important to control such clinical diseases.

The fluorescence method is superior for quantification of Hb level in blood, due to its high selectivity & sensitivity, good reproducibility with accuracy, rapid and simple[25,26] over other methods like high performance liquid chromatography[27], electrochemical methods[28–31], colorimetry[32,33] and chemiluminscence[34]. However, most of the fluorescence methods show relatively less selectivity and sensitivity due to the usage of transducer like metal complexes, dyes, SQDs (toxic). Then CQDs dominate the listed transducer by its unique properties[3]. The heme group in Hb can be adsorbed on CQDs surfaces via conjugated structure due to π-π interactions[24]. At the same time, the hydrophobicity of porphyrin in heme can interact with hydrophobic parts of cholesterol. Also, Fe^{2+} make a coordination complex with hydroxyl moiety of CQDs[24]. So we have prepared

hydroxyl-rich CQDs for selective, sensitive, accurate determination of Hb by fluorescence method.

In this work, we developed fluorescence probe i.e. CQDs synthesized from an unconventional precursor namely cholesterol under hydrothermal treatment at 180 °C for 8 hours. This method is very simple, inexpensive, selective and sensitive for determination of Hb with nanomolar level. Initially, we found two types of carbon materials in reaction mixture as carbon particles in solid portions and as CQDs in liquid portions that show excitation dependent and independent fluorescence emission respectively. These carbon materials were further characterized by spectroscopic and microscopic techniques. The solid portions displayed as large sized, amorphous carbon particles and liquid portions established as nano sized, crystalline, graphitic carbon quantum dots. Further, the optical properties of CQDs with respect to the concentration of precursor, reaction time & temperature were studied. The CQDs with maximum quantum yield is selected to further detailed studies. The effect of pH on optical properties of CQDs also discussed. Hemoglobin determination in commercial & human blood samples in presence of usual interfering molecules were studied using CQDs as a fluorescence probe.

2 Materials and Methods

2.1 Chemicals

Uric acid (UA), Cysteine (S-Cys), Cystine (SS-Cys), Folic acid (FA) were purchased from SRL, India. Cholesterol, Glutathione (GSH), Dopamine (DA), Homocysteine (H-Cys), Glucose (GOH), Vitamin B12 (VitB12), Dialysis tubing (2 kDa) purchased from Sigma-Aldrich. Hydrochloric acid (HCl), Sodium hydroxide (NaOH), Ascorbic Acid (AA) purchased from MERCK. All chemical were analytical grade and used without further purification. All solutions were prepared with Milli-Q water (18.2 MΩ.cm).

2.2 Synthesis of CQDs

0.5 g of cholesterol dissolved in 30 mL of a mixture of ethanol and water (1:5 ratio; 5 mL of ethanol and 25 mL of MilliQ water) and transferred to autoclave (50 mL capacity). Than 180 °C of temperature preserved for 8 h through the furnace with a heating rate of 3 °C/min. After 8 h the autoclave was allowed to cool room temperature. (We have synthesized a series of CQDs with different reaction time, temperature, the concentration of cholesterol to prepare CQDs. The prepared sample was purified with 0.2-μm syringe filter followed by 2 kDa cellulose dialysis tube. Then each composition was analyzed by UV-vis and PL spectroscopy. Finally, we selected CQDs synthesized from 0.5 g of cholesterol carbonized at 180 °C of temperature for 8 hours' time which has a high quantum yield (QY) i.e. 45.5%, Table S1). The purified sample used to further characterization techniques and adjusted to various pH levels using HCl and NaOH. The Quantum yield calculation, spectroscopy, microscopy techniques and sample preparation for analytical studies were described in supporting information, SI 1.

3 Results and Discussion

3.1 Optimization of CQDs

In optimization, to understanding the effect of temperature on the formation of CQDs, we dissolved 0.1 g of cholesterol each in two autoclaves containing 30 mL of ethanol: water mixture for carbonization reaction of 4 hours at 140 °C and 180 °C. The UV-vis and PL spectra of CQDs prepared from various reaction conditions are shown in Fig. S1a and S1b respectively. The CQDs which is formed at 180 °C gives high emission intensity (QY = 19.3 %). Thus 140 °C is not sufficient to complete carbonization. Further, to evaluate the effect of concentration of precursor (cholesterol) on the formation of CQDs, we prepared CQDs using 0.5 g, 1.0 g of cholesterol at 180 °C for 4 h. We found carbon particles as residue along with

CQDs as dispersion in autoclaves which were synthesized from 0.5 g and 1.0 g of cholesterol. The CQDs prepared from 0.5 g of cholesterol gives maximum QY (36.5 %) between those three CQDs (cholesterol concentration 0.1 g, 0.5 g, 1.0 g). In order to understand the reaction time, we prepared CQDs from 0.5 g of cholesterol with various reaction time i.e. 8 h, 12 h under heating of 180 °C. We found CQDs and carbon particles in each autoclave. The CQDs prepared from 8 h reaction time gives maximum fluorescence emission with QY of 45.5 %. The absorbance intensity of carbon particles has gradually increased with decreasing wavelength from 900 nm to 220 nm (Fig. S2). The PL spectra of carbon particles show the PL emission peaks shifted with excitation wavelengths ranging from 270 nm to 550 nm (Fig. S3). It is clearly indicating the presence of surface defects or the size/molecular fluorophores of carbon particles are not uniform. The carbon particles making a self-assembled chain-like network with neighbour particles and have a wide range of size from 440 nm to 750 nm (Fig. S4a). The absence of fringes and SAED pattern confirms that the carbon particles are amorphous carbon (Fig. S4b-c). The detailed description of carbon particles is given in supporting information (see SI. 2). The QY, reaction time & temperature, the concentration of precursor for CQDs optimization were tableted in Table 1. Finally, we have selected the CQDs by optimizing the synthesis condition i.e. 0.5 g of cholesterol carbonized at 180 °C for 8 h give maximum quantum yield.

3.2 Structural analysis

The FTIR spectra are shown in Fig. 1a, show the sharp peak at 3670 cm^{-1} assigned to free O-H stretching vibration[3]. The same vibrational mode is extended up to 3200 cm^{-1}, centered at 3445 cm^{-1} due to, a terminal hydrogen bond between dots. The peaks appear at 1244 cm^{-1} and 1042 cm^{-1} are assigned to C-O stretching and bending vibrations[3]. Further the peaks at 947 cm^{-1} and 1450 cm^{-1} assigned to O-H bending vibrations out of the plane and in-plane modes. From these results, we confirmed the presence of plenty of OH groups

present on surfaces of CQDs and involved to make a hydrogen bond with neighboring CQDs. The peaks appear at 1717 cm^{-1} and 1650 cm^{-1} are assigned to C=O and C=C stretching vibrations. The highest absorbance of C=C groups confirms that the CQDs was build up by conjugated C=C network like graphene[3]. These functional groups further investigated by XPS analysis. The survey spectrum of CQDs as shown in Fig. S5 that shows two peaks around at 286 eV and 532 eV due to C1s and O1s region. The deconvoluted C1s spectra in Fig. 1b shows three Gaussian peaks i.e. 284.6 eV, 285.9 eV, and 288.0 eV corresponds to sp^2 hybridized carbon (C-C, C=C), sp^3 hybridized carbon (C-O), and oxidized carbon (C=O) respectively. We don't observe any peak around at 289.9 eV due to carboxylic acid functional groups[3]. The O1s peak illustrated in Fig. 1c is best fitted with two Gaussian peaks at 531.0 eV and 532.7 eV. This peaks can be assigned to quinone type C=O and phenol C-O-H, ether C-O-C groups[35]. The H^1 NMR spectrum of CQDs given in Fig. S6a that shows two major peaks at 5.4 ppm and 7.2 ppm corresponds to sp^2 hybridized, phenolic OH and CH protons respectively. The peaks from 0.4 ppm to 2.2 ppm can be assigned to sp^3 hybridized CH and OH protons. The decreased chemical shift for the OH due to the absence/lack of electron withdrawing parts (possibly COOH), lack of intra molecular hydrogen bond and extended alkane chains at terminal[36]. The C^{13} NMR spectrum of CQDs in Fig. S6b shows that the presence of four type of sp^2 hybridized carbons such as C=O, C-OH, C=C, C-O-C corresponds to a chemical shift of 208, 142, 123 and 78 ppm. The peaks from 10-50 ppm can be assigned to sp^3 carbons. All sp^3 carbon groups can act as hydrophobic parts of CQDs. The sp^2 hybridized phenolic OH and ether groups can act as hydrophilic nature in structure. The amphiphilic groups offer us to use the CQDs in the wide application, for instance, biosensor. The FTIR, XPS and NMR results confirm the presence of sp^2 hybridized C=C, C-H groups are higher than OH groups. Moreover, the cholesterol is converted into CQDs as graphitic carbon network with terminal groups of hydrophilic-hydroxyl/ether functional groups and

hydrophobic-aliphatic carbon groups. Liu LQ et al explained that the fluorescence QY is higher in hydroxyl coated carbon dots than carboxylic coated carbon dots[37]. Compared with our previously reported work where CQD with hydroxyl, amino, carboxylic functionalized CQDs, higher QY in this report is due to plenty of hydroxyl groups on CQDs surface[3].

3.3 Optical studies

The UV-vis spectrum of CQDs is shown in Fig. 2a, which show shoulder absorption peak like a hump occurred at 230 nm due to n-σ* of phenolic hydroxyl or ether surface functional groups. The increasing absorbance from 500 nm to 300 nm corresponds to π-π* and n-π* transition of the intrinsic C=C and surface C=O functional groups. Fig. S7 shows PL spectra of CQDs at different excitation range from 230 nm to 390 nm with an interval of 20 nm. The maximum fluorescence emission intensity is observed at a wavelength of 440 nm while excitation is 250 nm and illustrated in Fig. 2c. The time-resolved fluorescence spectrum of CQDs fitted in a single exponential curve and lifetime of excited CQDs is 13.7 ns, derived from Fig. S8. This observation also proved the uniform size of CQDs with λ_{ex} independent, single fluorescence emission nature. Further, the fluorescence emission wavelength/intensity is unchanged for more than 6 months (Fig. S9). The stability and large Stokes shift encouraged us to differentiate the target from background signal in imaging applications even long-term studies. Additionally, the emission wavelength is not changed with changing of excitation wavelength which implies that the CQDs have same size and surface functional groups. Usually, oxygen-containing fluorescent carbon dots or oxidized carbon dots exhibit wavelength dependent fluorescence emission due to uneven size and/or surface defects[37,38]. These surface defects have been passivated by nitrogen, phosphorus, sulfur doping to get λ_{ex} independent fluorescence emission [9–11,22]. Xiaofang Jia et al reported the excitation dependent fluorescence emission in hydroxyl rich carbon dots

prepared from ascorbic acid by hydrothermal method[18]. But the un-doped, λ_{ex} -independent fluorescence emission in oxygen-containing CQDs is uncommon that we observed for first time. This means the hydroxyl/ether groups do not involve in exciton energy level of CQDs. The fluorescence originates from the single electronic transition of π-π conjugation at intrinsic carbon skeleton and not originate from surface functional groups. The observed single energy level in CQDs confirms that all CQDs are even size and do not have any surface defects.

3.4 Morphology analysis

The size, crystallinity of CQDs is investigated by HRTEM technique. The HRTEM images show the average size of CQDs is 9 nm (average of 7 dots) calculated from Fig. 3a and corresponding histogram as an inset of Fig. 3a. The d-spacing of CQDs measured from fringes in Fig. 3b is 0.228 nm. It can be assigned to (100) plane of the graphitic sp^2 carbon[3]. Further, the planes of CQDs also revealed the sp^2 graphitic carbon interrupted from SAED pattern as shown in Fig. 3c, i.e. 0.205 nm, 0.226 nm, 0.335 nm which can be assigned to (102), (100), (006) planes[3,39]. Ray et al reported the lattice spacing of 0.208 nm corresponds to diamond-like sp^3 carbon or graphite-like sp^2 carbon[39,40]. But our NMR, FTIR results proved maximum of sp^2 carbon. The nature of λ_{ex} –independent emission, short fluorescence lifetime (τ_0 = 13.7 ns), sp^2 graphitic carbon concluded that the formed one is CQDs among the various carbon dots such as carbon nanodots (sp^3, very short fluorescence lifetime), graphene quantum dots (relatively high fluorescence lifetime)[3].

3.5 Effect of pH

The CQDs were covered with a lot of hydroxyl groups which provide good water solubility and QY of 45 %. The fluorescence emission intensity & wavelength of CQDs at excitation/emission wavelengths of 250/440 nm, does not change much either in acidic or

basic pH conditions (Fig. S10). However, zeta potentials were changed when changing the pH of the medium using HCl and NaOH. The zeta potentials are 32.1 mV, -1.9 mV and -46.2 mV for pH at 2.0, 7.0 and 12.0 respectively. The pH of as prepared CQDs dispersion is 4.8, which implies that the prepared dots is acidic in nature like phenol. This also confirms the presence of extent of phenol like structures (hydroxyl functionalized graphite network). Thus functional groups (hydroxyl) present on CQDs surface are pH sensitive, but it will not affect the fluorescence emission. If the fluorescence arises from surface defects, the fluorescence may change with respect to medium pH. The change in the concentration of H^+ and OH^- may lead to the electronic transition variations of π-π* and n–π* in CQDs containing C=O, C=N, C=S, C=P auxochrome groups by refilling or depleting their valence band. We have C=O in their structure which also undergoes protonation/deprotonation, thus zeta potential changed. But the fluorescence has not affected, thus indicating that the fluorescence does not arise from the electronic transition of π-π* and n–π* of auxochrome/fluorophores. Considering pH – independent, λ_{ex} – independent emission, the fluorescence originates from quantum/size confinement effect, not from the surface defects/states or any other fluorophores. In our previous work, we report the pH dependent fluorescence emission in carboxylic acid, amine, and hydroxyl functionalized carbon quantum dots[3]. In this case the fluorescence originates from intrinsic core of CQDs which contain pH sensitive auxochromes. Here, we established that the hydroxyl groups in CQDs are pH sensitive but not acting as auxochromes. So we can use this probe for a biological application like fluorometric analysis and imaging at any pH levels.

The FTIR, XPS, UV-vis, PL, NMR and HRTEM results clearly confirmed that the formed one is amphiphilic, very stable, pH & λ_{ex} – independent emissive, graphitic carbon quantum dots with surface functional groups of hydroxyl, ether and keto groups.

3.6 Determination of hemoglobin

To evaluate whether the concentration of Hb can be determined using CQDs as fluorescence probe, 20 µM of Hb was added in the CQDs dispersion. The fluorescence emission intensity was quenched about 90 % at excitation/emission wavelengths of 250/440 nm (Fig. 2d). Further, the emission intensities recorded through PL spectra in same wavelengths for the Hb concentration range from 100 nM to 20 µM (Fig. 4a) and it is gradually decreased. Commonly the hemoglobin can adsorb onto the surfaces of carbon-based nanomaterials over hydrophobic areas[25,41]. The adsorption of hemoglobin on CQDs leads to fluorescence quenching effect. The Stern-Volmer quenching constant (K_{sv}), bimolecular quenching rate constant (k_q) and binding constant (K) can be derived from Stern-Volmer equation **(Eq. 1)** and Lineweaver–Burk equation **(Eq. 2)** respectively[3].

$$\frac{F_0}{F} = 1 + K_{SV}[Q] = 1 + k_q \tau_0 [Q] \qquad \text{..... (Eq. 1)}$$

$$\frac{1}{F_0 - F} = \frac{1}{F_0} + \frac{1}{KF_0}\frac{1}{[Q]} \qquad \text{..... (Eq. 2)}$$

Where F and F_0 are the fluorescence intensity of the CQDs in presence and absence of hemoglobin. $\tau_{0,}$ and [Q] are the excited state lifetime of CQDs in the absence of Hb, and hemoglobin concentration respectively. The K_{sv} value calculated from Stern-Volmer plot (Fig. S11a) that is 8.61×10^7 M^{-1}. The k_q is 6.28×10^{15} $M^{-1}s^{-1}$ calculated from **Eq. 1** (excited state lifetime of CQDs in the absence of hemoglobin, τ_0 is 13.7 ns from Fig. S8). The binding constant, K is 7.09×10^7 M^{-1} for CQDs-Hb system (calculated from Fig. S11b). Other researchers have found that the Stern-Volmer quenching constant, K_{sv}, can be represented by a first associative binding constant[42]. The K_{sv} for hemoglobin with electrochemically synthesized carbon nanodots is 1.6×10^6 M^{-1}[41], with cytylpyridinum chloride ions is about 10^4 M^{-1}[42], with CdS quantum dots is 10^7 M^{-1}[43], and with the gold nanodots is 1.6×10^7 M^{-1}[44]. We have reported that the K_{sv} is 3.01×10^7 M^{-1} and K is 2.34×10^7 M^{-1} for hemoglobin determination using polyaniline sulfonic acid stabilized gold nanoclusters[25].

Therefore the higher value of binding constant occurred by strong adsorption that attributed to hydrophobic interaction. Usually, hemoglobin adsorbed on graphitized carbon-based nanomaterials by π -π interactions. But the hydrophobic interactions stronger than π -π interactions. Bui TT et al described that selective determination of cholesterol using Hb functionalized carbon dots via hydrophobic interactions between Hb and cholesterol[24]. Moreover, the Fe^{2+} may coordinate with the hydroxyl moiety of CQDs. These factors lead to make strong affinity complex as a result, higher binding constant value and static quenching can happen. The fluorescence quenching mechanism can be explained by inner filter effect (IFE)[23], i.e. reduction of fluorescence emission intensity due to filtering off emission of the particle by a second absorber or fluorescence resonance energy transfer (FRET)[41] for Hb system. The IFE can be possible at distance between CQDs and Hb is exceed 10 nm. The higher binding constant value due to strong adsorption says that the distance between CQDs and Hb cannot be higher than 10 nm[3,45] and IFE is not possible here. According to Forster non-radiative energy transfer theory, the energy transfer can occur under three main circumstances, i.e. (i) dipole-dipole interactions between CQDs and Hb, (ii) spectral overlap between the emission spectrum of CQDs and the absorbance spectrum of Hb (iii) distance between CQDs and Hb is 1-10 nm. The FRET process is confirmed by the dipole interactions between Fe^{2+} and hydroxyl groups, the absorbance spectrum of Hb overlapped with the emission spectrum of CQDs (Fig. 2b and 2c), less than 10 nm distances between CQDs and Hb. The changes in the efficiency of FRET with respect to the concentration of hemoglobin is shown in Fig. 4b. The efficiency is linearly increased from 100 nM to 2.9 µM with correlation coefficient of 0.987 and follows linear regression equation as $y = 0.00025x + 0.06043$ (Fig. 4b inset). From the plot, the limit of detection (LOD) and limit of quantification calculated as 24 nM and 80 nM based on the triple standard deviation of CQDs fluorescence intensity in the absence of Hb. After 2.9 µM, the efficiency is not changed much

due to no more CQDs available to give fluorescence. The efficiency of FRET to be calculated as 76.7 % and 94.2 % for 2.9 and 20 µM of Hb (see SI 1.2). Therefore, our fluorescence probe is best for determination of hemoglobin up to 2.9 µM. Other analytical methods for determination of hemoglobin with LOD, linear range were tabled as Table. 2.

Fig. 5 shows, the PL intensities of CQDs in presence of 1 mM of various biological interfering molecules such as GSH, S-Cys, RF, UA, AA, DA, VB_{12}, SS-Cys, GOH, H-Cys and 20 µM of hemoglobin. These biomolecules don`t show significant changes in PL intensity. Generally, metal ions easily bound with hydroxyl moiety of CQDs via coordination bonds[37]. The Cr^{4+} ions reduce the fluorescence of graphene quantum dots by Cr-GQDs complex formation. Then the fluorescence recovered by AA via Cr-AA complex formation[48]. Similarly, Cu^{2+} blocked the fluorescence of S, N-doped carbon dots and unblocked by S-Cys, H-Cys and GSH[49]. From these reports, the AA, S-Cys, GSH, and H-Cys will not directly interact with CQDs, so the fluorescence will not change and we don't have metal ion containing molecule except VB_{12}. The VB_{12} molecule (cyanocobalamin-Cobalt (II) ion coordinated by four nitrogen of the corrin rings) which is structurally similar to hemoglobin may affect the fluorescence intensity of CQDs. But the intensity has not changed much due to weakened spectral overlap between CQDs and VB_{12}, thus FRET cannot be possible. Hence our method is reliable for determination of hemoglobin in presence of biological interfering molecules. The high selectivity towards Hb induces us to make studies on human blood samples.

3.7 Determination of hemoglobin in human blood

We have collected blood samples with its actual concentration of Hb (determined by immunoturbidimetric assay) from CSIR-CECRI health center. We are following the sample preparation procedure described by Huan-Tsung Chang group[44]. The 1 mL of blood

samples was diluted tenfold with MilliQ water in sterilized vials. The vials were sonicated for 30 s to erythrocyte lysis. After lysis, the samples were centrifuged at RCF 1000 g, 4 ºC for 20 min. The human serum albumin (possible interference) settled down as residue and the supernatants were taken for the analyses of hemoglobin determination. We followed standard addition method for detection of Hb in human blood samples that minimize the matrix interference. The standard Hb (100 nM – 1000 nM) spiked in the mixtures of diluted supernatants samples (1000-fold dilution, 1 mL) and CQDs (1 mL) to make their final volumes of 3 mL. Then the mixtures were kept under room temperature for 30 min preceding to the analysis in a quartz cuvette and the PL intensities recorded at excitation/emission wavelengths of 250/440 nm. The average of the three replicates of Hb determination by a proposed method well agreed with those values obtained by the immunoturbidimetric assay and the value is tabulated in Table. 3. The normal range of the Hb concentrations is 1.706 mM to 2.714 mM in human blood[44]. The concentration of hemoglobin in three human blood samples was calculated to be 1.664 mM, 1.405 mM and 1.748 mM from Fig. S12a-c by considering the dilution factor (10^4-fold dilution). The slope values of standard addition method i.e. 2.7×10^{-4} – 2.8×10^{-4} very near to slope value of the calibration curve method i.e. 2.5×10^{-4}. This result indicating that the matrix components do not interfere with hemoglobin determination on diluted blood samples. Compare to the Immunoturbidimetric assay, our method is simple and inexpensive. Moreover, a single drop of blood sample enough that can be taken from fingertips of the patient, no need to collect from a vein (Immunoturbidimetric assay).

4 Conclusions

The highly stable, amphiphilic, graphitized carbon quantum dots were prepared from cholesterol under hydrothermal condition. The CQDs have many features like λ_{ex} & pH-independent fluorescence emission with high quantum yield (QY= 45 %). The hydroxyl-rich

surfaces of CQDs offer us an easy route for the determination of hemoglobin in commercial and diluted human blood samples. The detection principle is explained by experimental evidence as FRET between CQDs and Hb due to strong adsorption via dipole-dipole interactions, π-π interactions, and hydrophobic interactions. The Stern-Volmer quenching constant and binding constant values correspond to strong adsorption leading to FRET process. The efficiency of FRET linearly increased in the range of 100 nM – 2.9 µM and limit of detection is calculated to be 24 nM (signal to noise ratio is 3.0). The CQDs as fluorescence probe can detect hemoglobin in human blood samples through standard addition method which is comparable to the standard Immuno-turbidimetric assay. Therefore this simple method suggested the sensitive and selective determination of Hb in the field of diagnosis of numerous diseases including anemia, erythrocytosis, and thalassemias.

Acknowledgement

Gopi Kalaiyarasan thank, joint CSIR-UGC, New Delhi for the award of Junior Research Fellowship.

References

[1] S.Y. Lim, W. Shen, Z. Gao, Carbon quantum dots and their applications., Chem. Soc. Rev. 44 (2014) 362–381. doi:10.1039/c4cs00269e.

[2] N. Dhenadhayalan, K.-C. Lin, Chemically Induced Fluorescence Switching of Carbon-Dots and Its Multiple Logic Gate Implementation, Sci. Rep. 5 (2015) 10012. doi:10.1038/srep10012.

[3] G. Kalaiyarasan, J. Joseph, Determination of vitamin B12 via pH-dependent quenching of the fluorescence of nitrogen doped carbon quantum dots, Microchim. Acta. 184 (2017) 3883–3891. doi:10.1007/s00604-017-2421-y.

[4] H. Li, Z. Kang, Y. Liu, S.-T. Lee, Carbon nanodots: synthesis, properties and applications, J. Mater. Chem. 22 (2012). doi:10.1039/c2jm34690g.

[5] L. Sun, P. Gong, X. Liu, M. Pang, M. Tian, J. Chen, J. Du, Z. Liu, Fluorinated carbon fiber as a novel nanocarrier for cancer chemo-photothermal therapy, J. Mater. Chem. B. 5 (2017) 6128–6137. doi:10.1039/C7TB01155E.

[6] P. Gong, Q. Zhao, D. Dai, S. Zhang, Z. Tian, L. Sun, J. Ren, Z. Liu, Functionalized Ultrasmall Fluorinated Graphene with High NIR Absorbance for Controlled Delivery of Mixed Anticancer Drugs, Chem. - A Eur. J. 23 (2017) 17531–17541. doi:10.1002/chem.201702917.

[7] P. Gong, S. Ji, J. Wang, D. Dai, F. Wang, M. Tian, L. Zhang, F. Guo, Z. Liu, Fluorescence-switchable ultrasmall fluorinated graphene oxide with high near-infrared absorption for controlled and targeted drug delivery, Chem. Eng. J. 348 (2018) 438–446. doi:10.1016/j.cej.2018.04.193.

[8] P. Gong, L. Guo, M. Pang, D. Wang, L. Sun, Z. Tian, J. Li, Y. Zhang, Z. Liu, Nano-sized paramagnetic and fluorescent fluorinated carbon fiber with high NIR absorbance for cancer chemo-photothermal therapy, J. Mater. Chem. B. 6 (2018) 3068–3077. doi:10.1039/c7tb03320f.

[9] W. Wang, Y.C. Lu, H. Huang, A.J. Wang, J.R. Chen, J.J. Feng, Facile synthesis of N, S-codoped fluorescent carbon nanodots for fluorescent resonance energy transfer recognition of methotrexate with high sensitivity and selectivity, Biosens. Bioelectron. 64 (2015) 517–522. doi:10.1016/j.bios.2014.09.066.

[10] W. Wang, Y.C. Lu, H. Huang, A.J. Wang, J.R. Chen, J.J. Feng, Solvent-free synthesis of sulfur- and nitrogen-co-doped fluorescent carbon nanoparticles from glutathione for highly selective and sensitive detection of mercury(II) ions, Sensors Actuators, B

Chem. 202 (2014) 741–747. doi:10.1016/j.snb.2014.06.010.

[11] W. Wang, Y.-C. Lu, H. Huang, J.-J. Feng, J.-R. Chen, A.-J. Wang, Facile synthesis of water-soluble and biocompatible fluorescent nitrogen-doped carbon dots for cell imaging, Analyst. 139 (2014) 1692–1696. doi:10.1039/C3AN02098C.

[12] J. Zhou, C. Booker, R. Li, X. Zhou, T.-K. Sham, X. Sun, Z. Ding, An electrochemical avenue to blue luminescent nanocrystals from multiwalled carbon nanotubes (MWCNTs)., J. Am. Chem. Soc. 129 (2007) 744–5. doi:10.1021/ja0669070.

[13] L. Zheng, Y. Chi, Y. Dong, J. Lin, B. Wang, Electrochemiluminescence of water-soluble carbon nanocrystals released electrochemically from graphite, J. Am. Chem. Soc. 131 (2009) 4564–4565. doi:10.1021/ja809073f.

[14] J. Wang, C.-F. Wang, S. Chen, Amphiphilic egg-derived carbon dots: rapid plasma fabrication, pyrolysis process, and multicolor printing patterns., Angew. Chem. Int. Ed. Engl. 51 (2012) 9297–301. doi:10.1002/anie.201204381.

[15] L. Guo, L. Li, M. Liu, Q. Wan, J. Tian, Q. Huang, Y. Wen, S. Liang, X. Zhang, Y. Wei, Bottom-up preparation of nitrogen doped carbon quantum dots with green emission under microwave-assisted hydrothermal treatment and their biological imaging, Mater. Sci. Eng. C. 84 (2018) 60–66. doi:10.1016/j.msec.2017.11.034.

[16] X. Lu, Z. Zhang, Q. Xia, M. Hou, C. Yan, Z. Chen, Y. Xu, R. Liu, Glucose functionalized carbon quantum dot containing organic radical for optical/MR dual-modality bioimaging, Mater. Sci. Eng. C. 82 (2018) 190–196. doi:10.1016/J.MSEC.2017.08.074.

[17] H. Li, X. He, Y. Liu, H. Huang, S. Lian, S.T. Lee, Z. Kang, One-step ultrasonic synthesis of water-soluble carbon nanoparticles with excellent photoluminescent

properties, Carbon N. Y. 49 (2011) 605–609. doi:10.1016/j.carbon.2010.10.004.

[18] X. Jia, J. Li, E. Wang, One-pot green synthesis of optically pH-sensitive carbon dots with upconversion luminescence, Nanoscale. 4 (2012) 5572. doi:10.1039/c2nr31319g.

[19] Z.-C. Yang, M. Wang, A.M. Yong, S.Y. Wong, X.-H. Zhang, H. Tan, A.Y. Chang, X. Li, J. Wang, Intrinsically fluorescent carbon dots with tunable emission derived from hydrothermal treatment of glucose in the presence of monopotassium phosphate, Chem. Commun. 47 (2011) 11615. doi:10.1039/c1cc14860e.

[20] S. Sahu, B. Behera, T.K. Maiti, S. Mohapatra, Simple one-step synthesis of highly luminescent carbon dots from orange juice: application as excellent bio-imaging agents., Chem. Commun. (Camb). 48 (2012) 8835–7. doi:10.1039/c2cc33796g.

[21] P. Gong, J. Wang, K. Hou, Z. Yang, Z. Wang, Z. Liu, X. Han, S. Yang, Small but strong: The influence of fluorine atoms on formation and performance of graphene quantum dots using a gradient F-sacrifice strategy, Carbon N. Y. 112 (2017) 63–71. doi:10.1016/j.carbon.2016.10.091.

[22] M. Zhang, C. Chi, P. Yuan, Y. Su, M. Shao, N. Zhou, A hydrothermal route to multicolor luminescent carbon dots from adenosine disodium triphosphate for bioimaging, Mater. Sci. Eng. C. 76 (2017) 1146–1153. doi:10.1016/J.MSEC.2017.03.144.

[23] A. Barati, M. Shamsipur, H. Abdollahi, Hemoglobin detection using carbon dots as a fluorescence probe, Biosens. Bioelectron. 71 (2015) 470–475. doi:10.1016/j.bios.2015.04.073.

[24] T.T. Bui, S.-Y. Park, A carbon dot–hemoglobin complex-based biosensor for cholesterol detection, Green Chem. 18 (2016) 4245–4253. doi:10.1039/C6GC00507A.

[25] G. Kalaiyarasan, A.V. Narendra Kumar, C. Sivakumar, J. Joseph, Photoluminescence of oligomers of aniline-2-sulfonic acid formed in the presence of AuCl4− and sodium citrate: Application in the optical detection of hemoglobin, Sensors Actuators B Chem. 209 (2015) 883–888. doi:10.1016/j.snb.2014.12.041.

[26] G. Kalaiyarasan, A. K, J. Joseph, Melamine dependent fluorescence of glutathione protected gold nanoclusters and ratiometric quantification of melamine in commercial cow milk and infant formula, Appl. Surf. Sci. 420 (2017) 963–969. doi:10.1016/j.apsusc.2017.05.193.

[27] Y. Li, L. Sun, J. Qian, C. Wang, Q. Liu, E. Han, N. Hao, L. Zhang, J. Cai, K. Wang, A homogeneous assay for highly sensitive detection of CaMV35S promoter in transgenic soybean by förster resonance energy transfer between nitrogen-doped graphene quantum dots and Ag nanoparticles, Anal. Chim. Acta. 948 (2016) 90–97. doi:10.1016/j.aca.2016.10.031.

[28] R. Zhang, S. Xu, J. Luo, X. Liu, Molecularly imprinted photo-sensitive polyglutamic acid nanoparticles for electrochemical sensing of hemoglobin, Microchim. Acta. 182 (2015) 175–183. doi:10.1007/s00604-014-1315-5.

[29] Y. Xian, Y. Zhou, Y. Xian, L. Zhou, H. Wang, L. Jin, Preparation of poly(vinylpyrrolidone)-protected Prussian blue nanoparticles-modified electrode and its electrocatalytic reduction for hemoglobin, Anal. Chim. Acta. 546 (2005) 139–146. doi:10.1016/j.aca.2005.04.090.

[30] H. Ju, H. Sun, H. Chen, Properties of poly-β-aminoanthraquinone modified carbon fiber electrode as a basis for hemoglobin biosensors, Anal. Chim. Acta. 327 (1996) 125–132. doi:10.1016/0003-2670(96)00067-0.

[31] D.M. Gao, Y. Sun, Q. Zhao, J.B. Hu, Q.L. Li, Determination of hemoglobin at a novel

NH 2 = ITO ion implantation modified electrode, Microchim. Acta. (2008) 241–246. doi:10.1007/s00604-007-0833-9.

[32] N. Pourreza, H. Golmohammadi, Hemoglobin detection using curcumin nanoparticles as a colorimetric chemosensor, RSC Adv. 5 (2015) 1712–1717. doi:10.1039/C4RA10386F.

[33] R. Li, Q. Jiang, H. Cheng, G. Zhang, M. Zhen, D. Chen, J. Ge, L. Mao, C. Wang, C. Shu, G-quadruplex DNAzymes-induced highly selective and sensitive colorimetric sensing of free heme in rat brain, Analyst. 139 (2014) 1993–1999. doi:10.1039/C3AN02025H.

[34] Z.S. Traore, S.M. Shah, X. Su, Flow-injection chemiluminescence determination of haemoglobin in the blood, Luminescence. 28 (2013) 56–62. doi:10.1002/bio.2337.

[35] D. Qu, M. Zheng, L. Zhang, H. Zhao, Z. Xie, X. Jing, R.E. Haddad, H. Fan, Z. Sun, Formation mechanism and optimization of highly luminescent N-doped graphene quantum dots, Sci. Rep. 4 (2015) 5294. doi:10.1038/srep05294.

[36] P. Charisiadis, V.G. Kontogianni, C.G. Tsiafoulis, A.G. Tzakos, M. Siskos, I.P. Gerothanassis, 1H-NMR as a structural and analytical tool of intra- and intermolecular hydrogen bonds of phenol-containing natural products and model compounds, Molecules. 19 (2014) 13643–13682. doi:10.3390/molecules190913643.

[37] L. Liu, Y. Li, L. Zhan, Y. Liu, C. Huang, One-step synthesis of fluorescent hydroxyls-coated carbon dots with hydrothermal reaction and its application to optical sensing of metal ions, Sci. China Chem. 54 (2011) 1342–1347. doi:10.1007/s11426-011-4351-6.

[38] H. Li, X. He, Z. Kang, H. Huang, Y. Liu, J. Liu, S. Lian, C.H. a Tsang, X. Yang, S.T. Lee, Water-soluble fluorescent carbon quantum dots and photocatalyst design, Angew.

Chemie - Int. Ed. 49 (2010) 4430–4434. doi:10.1002/anie.200906154.

[39] S.N. Baker, G. a. Baker, Luminescent carbon nanodots: Emergent nanolights, Angew. Chemie - Int. Ed. 49 (2010) 6726–6744. doi:10.1002/anie.200906623.

[40] S.C. Ray, A. Saha, N.R. Jana, R. Sarkar, Fluorescent Carbon Nanoparticles: Synthesis, Characterization, and Bioimaging Application, J. Phys. Chem. C. 113 (2009) 18546–18551. doi:10.1021/jp905912n.

[41] C.-I. Wang, W.-C. Wu, A.P. Periasamy, H.-T. Chang, Electrochemical synthesis of photoluminescent carbon nanodots from glycine for highly sensitive detection of hemoglobin, Green Chem. 16 (2014) 2509. doi:10.1039/c3gc42325e.

[42] A.-K. Bordbar, A. Taheri-Kafrani, Binding and fluorescence study on interaction of human serum albumin (HSA) with cetylpyridinium chloride (CPC)., Colloids Surf. B. Biointerfaces. 55 (2007) 84–89. doi:10.1016/j.colsurfb.2006.11.012.

[43] X.-C. Shen, X.-Y. Liou, L.-P. Ye, H. Liang, Z.-Y. Wang, Spectroscopic studies on the interaction between human hemoglobin and CdS quantum dots, J. Colloid Interface Sci. 311 (2007) 400–406. doi:10.1016/j.jcis.2007.03.006.

[44] L.-Y. Chen, C. Huang, W. Chen, H. Lin, H. Chang, Using photoluminescent gold nanodots to detect hemoglobin in diluted blood samples, Biosens. Bioelectron. 43 (2013) 38–44. doi:10.1016/j.bios.2012.11.034.

[45] E. Vaishnavi, R. Renganathan, CdTe quantum dot as a fluorescence probe for vitamin B12 in dosage form, Spectrochim. Acta - Part A Mol. Biomol. Spectrosc. 115 (2013) 603–609. doi:10.1016/j.saa.2013.06.068.

[46] S. Pang, S. Liu, X. Su, A novel fluorescence assay for the detection of hemoglobin based on the G-quadruplex/hemin complex., Talanta. 118 (2014) 118–22.

doi:10.1016/j.talanta.2013.10.004.

[47] F. Morgner, A. Lecointre, L.J. Charbonnière, H.-G. Löhmannsröben, Detecting free hemoglobin in blood plasma and serum with luminescent terbium complexes, Phys. Chem. Chem. Phys. 17 (2015) 1740–1745. doi:10.1039/C4CP04206A.

[48] S. Huang, H. Qiu, F. Zhu, S. Lu, Q. Xiao, Graphene quantum dots as on-off-on fluorescent probes for chromium(VI) and ascorbic acid, Microchim. Acta. 182 (2015) 1723–1731. doi:10.1007/s00604-015-1508-6.

[49] Y. Guo, L. Yang, W. Li, X. Wang, Y. Shang, B. Li, Carbon dots doped with nitrogen and sulfur and loaded with copper(II) as a “turn-on” fluorescent probe for cystein, glutathione and homocysteine, Microchim. Acta. 183 (2016) 1409–1416. doi:10.1007/s00604-016-1779-6.

Table. 1. The experimental conditions and quantum yield for synthesized carbon quantum dots.

Concentration of cholesterol, (g)	Reaction temperature, (°C)	Reaction time, (h)	Quantum yield, (%)
0.1	140	4	14.5
0.1	180	4	19.3
0.5	180	4	36.5
1.0	180	4	21.3
0.5	180	8	45.5
0.5	180	12	38.9

Table. 2 Comparison of available methods for determination of hemoglobin.

Method	Probe	LOD, (M)	Linear range, (M)	Ref.
Fluorimetry	Carbon dots and H_2O_2	4.0×10^{10}	1.0×10^{-9}-1.0×10^{-7}	[23]
Fluorimetry	G-quadruplex/hemin complex	2.0×10^{-9}	5.0×10^{-9}-2.0×10^{-7}	[46]
Fluorimetry	Luminescent terbium complexes	-	7.7×10^{-7}-6.2×10^{-5}	[47]
Fluorimetry	Aniline-2-sulfonic acid stabilised gold clusters	-	1.0×10^{-8}-1.0×10^{-5}	[25]
Colorimetry	G-quadruplex-DNAzymes	6.4×10^{-10}	1.0×10^{-9}-1.2×10^{-7}	[33]
Colorimetry	Curcumin nanoparticle	1.5×10^{-9}	1.5×10^{-8}-6.2×10^{-7}	[32]
Fluorimetry	Gold nanodots	5.0×10^{-10}	1.0×10^{-9}-1.0×10^{-8}	[44]
Cyclic voltammetry	Poly-β-aminoanthraquinone modified carbon fiber electrode	-	1.0×10^{-6}-4.0×10^{-4}	[30]
Amperometry	Poly-β-aminoanthraquinone	-	5.0×10^{-7}-	[30]

	modified carbon fiber electrode		3.4×10^{-4}	
DPSV	Poly glutamic acid nanoparticles	-	7.8×10^{-8}-1.5×10^{-6}	[28]
DPV and Amperometry	poly(vinylpyrrolidone) protected Prussian blue nanoparticles	4.0×10^{-8}	1.0×10^{-7}-1.2×10^{-5}	[29]
Cyclic voltammetry	Gold nanoparticles/NH_2/ITO	1.0×10^{-8}	1.0×10^{-8}-1.0×10^{-6}	[31]
Fluorimetry	Carbon quantum dots	2.4×10^{-8}	1.0×10^{-7}-2.0×10^{-5}	This work

DPSV-Differential Pulse Stripping Voltammetry, DPV-Differential Pulse Voltammetry, ITO-Indium doped tin oxide

Table. 3 Determination of hemoglobin in human blood samples by a commercial method (Immunoturbidimetric assay) and our method.

Sample	Immunoturbidimetric assay, (mM)	Proposed method, (mM)	Recovery, (%)
Patient 1	1.737	1.664	95.7
Patient 2	1.551	1.405	90.5
Patient 3	1.923	1.748	90.8

Highlights

1. Amphiphilic, graphitic CQDs prepared from cholesterol by hydrothermal method.
2. Fluorescence arise from intrinsic/extrinsic core in small/large dots respectively.
3. Excitation independent fluorescence emission in oxygen only contained CQDs is new.
4. CQDs are hydrophilic due to hydroxyl and hydrophobic due to alkane rings.
5. Fluorometric determination of hemoglobin in diluted human blood samples reported.

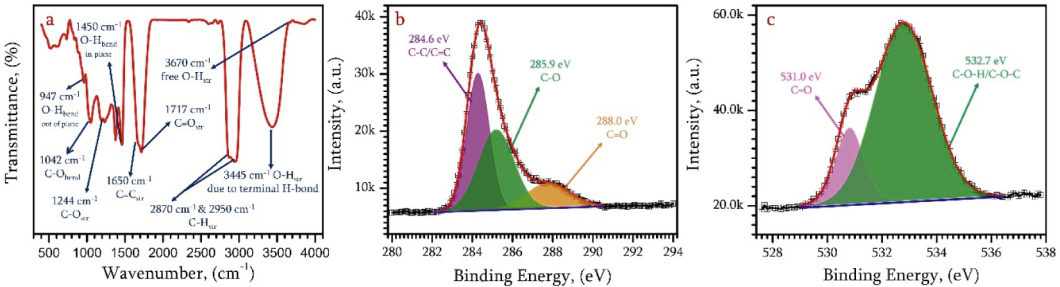
a
1450 cm-1
O-Hbend
in plane
3670 cm-1
free O-Hstr
947 cm-1
O-Hbend
out of plane
1717 cm-1
C=Ostr
1042 cm-1
C-Obend
1650 cm-1
C=Cstr
3445 cm-1 O-Hstr
due to terminal H-bond
1244 cm-1
C-Ostr
2870 cm-1 & 2950 cm-1
C-Hstr
Transmittance, (%)
Wavenumber, (cm-1)
b
284.6 eV
C-C/C=C
285.9 eV
C-O
288.0 eV
C=O
Intensity, (a.u.)
Binding Energy, (eV)
c
531.0 eV
C=O
532.7 eV
C-O-H/C-O-C
Intensity, (a.u.)
Binding Energy, (eV)

Figure 1

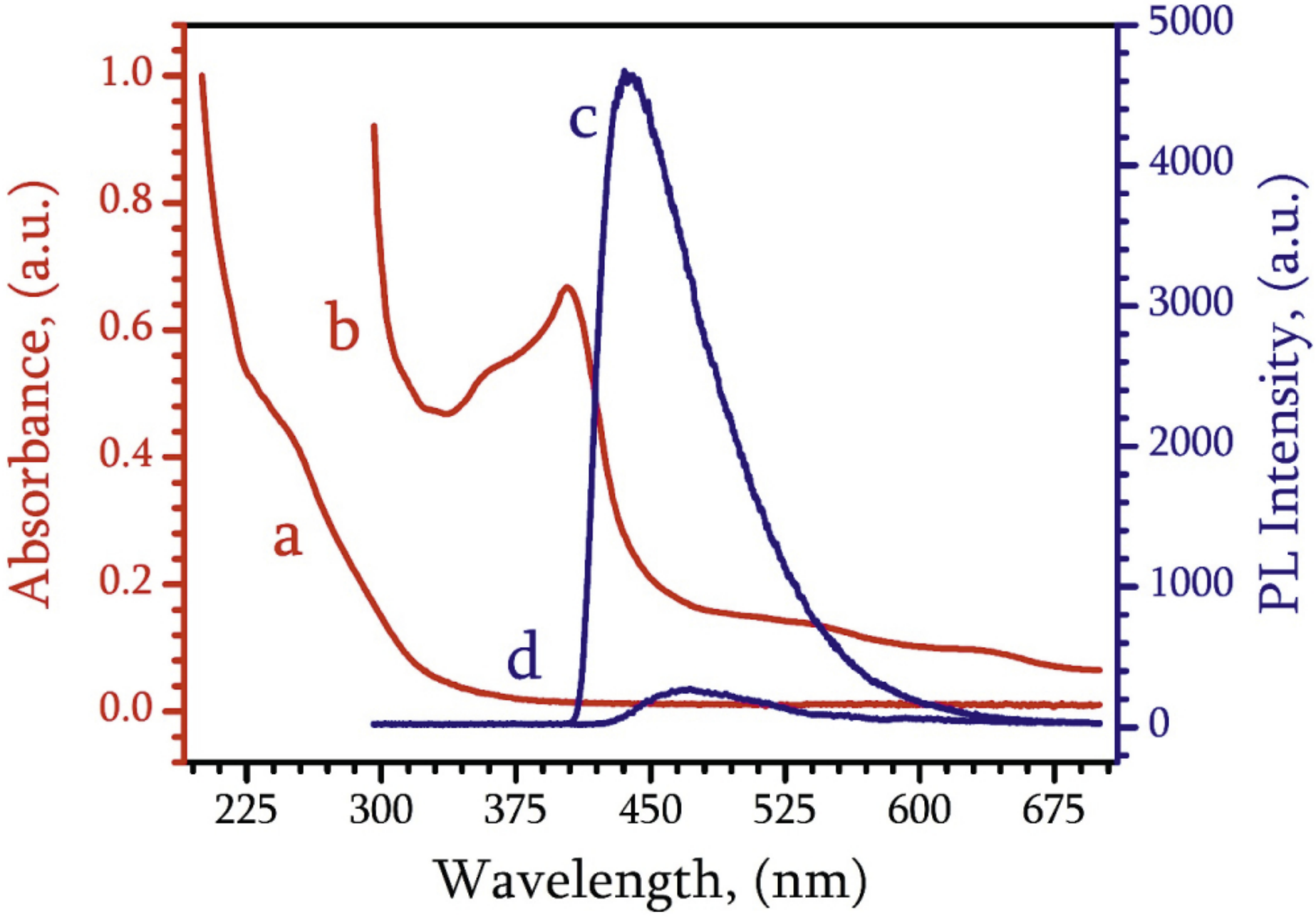
Absorbance, (a.u.)
1.0
0.8
0.6
0.4
0.2
0.0
PL Intensity, (a.u.)
5000
4000
3000
2000
1000
0
225
300
375
450
525
600
675
Wavelength, (nm)
a
b
c
d

Figure 2

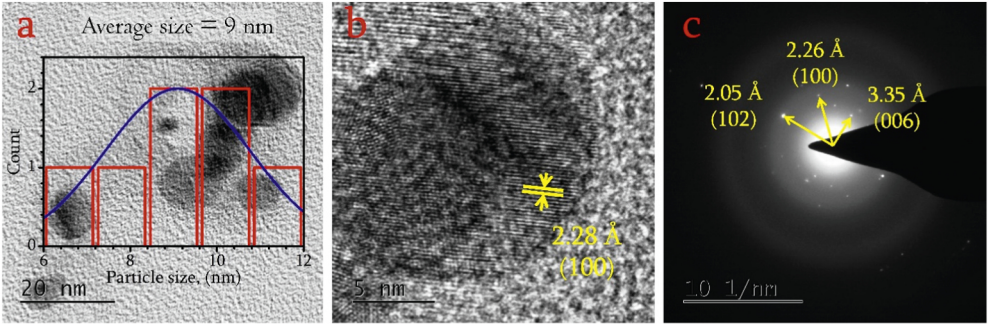
a
Average size = 9 nm
Count
Particle size, (nm)
20 nm
b
2.28 Å
(100)
5 nm
c
2.26 Å
(100)
2.05 Å
(102)
3.35 Å
(006)
1.0 1/nm

Figure 3

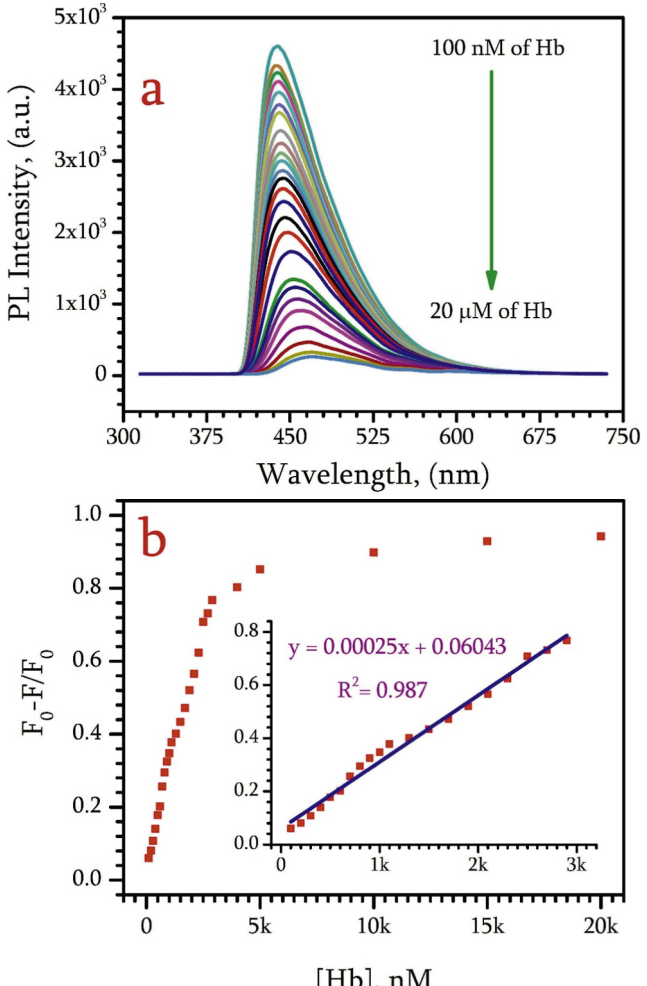
a
100 nM of Hb
20 μM of Hb
PL Intensity, (a.u.)
5x10^3
4x10^3
3x10^3
2x10^3
1x10^3
0
300
375
450
525
600
675
750
Wavelength, (nm)
b
F0-F/F0
1.0
0.8
0.6
0.4
0.2
0.0
y = 0.00025x + 0.06043
R^2= 0.987
0
1k
2k
3k
0
5k
10k
15k
20k
[Hb], nM

Figure 4

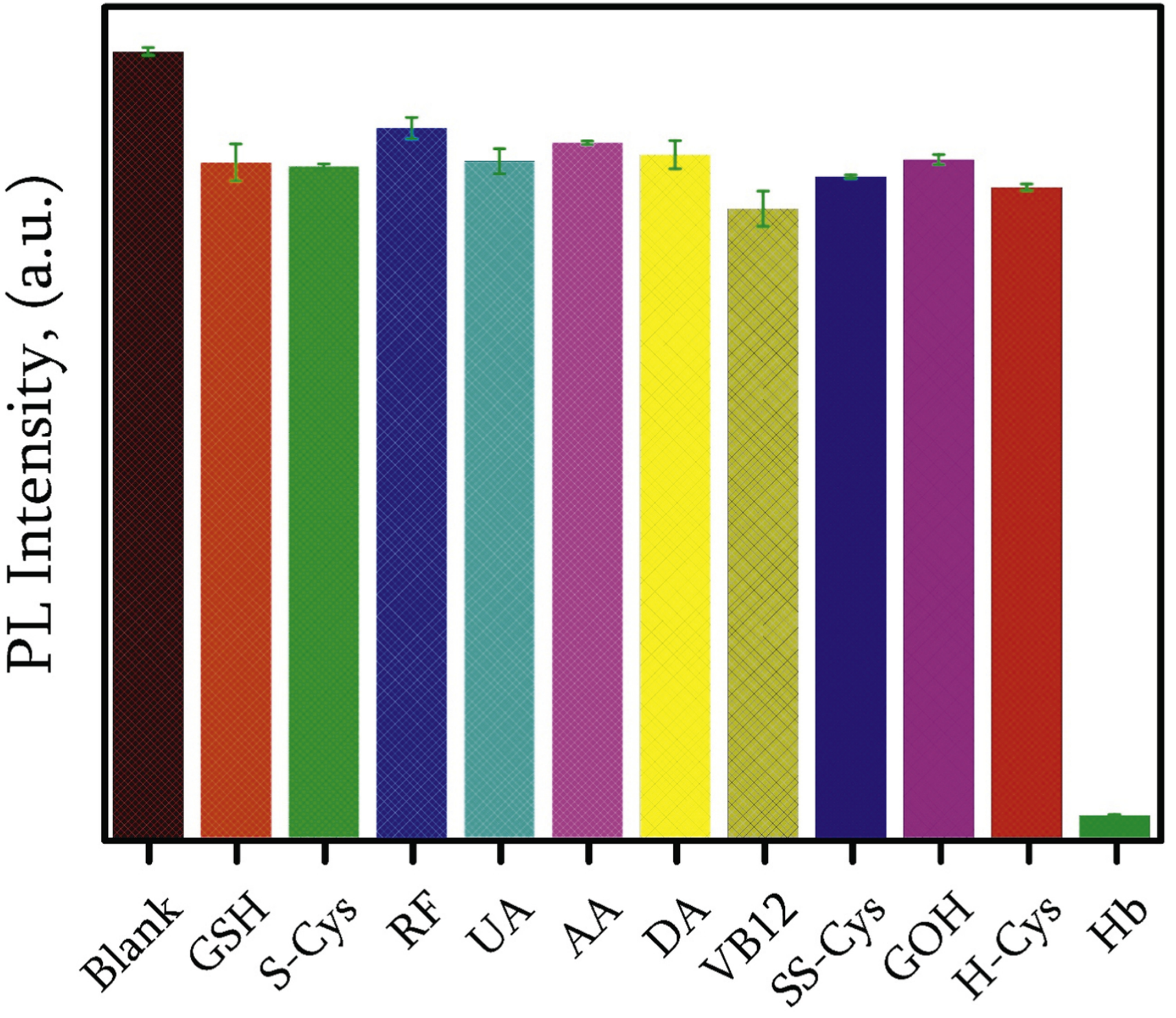
PL Intensity, (a.u.)
Blank
GSH
S-Cys
RF
UA
AA
DA
VB12
SS-Cys
GOH
H-Cys
Hb

Figure 5